

MECHANICAL ENGINEERING SENIOR DESIGN (2012-2013)

Team 20: Solar Powered Phase Change Compressor

Final Design Report

Addison Bender

Jesse Diaz

Emmanuel Ferdinand

Project Sponsor: Grant Peacock

Project Advisor: Dr. Juan Ordonez

Senior Design Coordinators: Dr. Kamal Amin, Dr. Chiang Shih

4/25/2013

Abstract

Steam generation from solar energy has the potential to be a cost effective and environmentally sustainable power source. The motivation of the solar powered phase change compressor was to create a functioning prototype of a compressor that could be retrofitted to a small load A/C unit. The concept of the design is meant to provide an alternative process to produce air conditioning without relying on conventional fossil fuel generated electricity.

A reciprocating diaphragm compressor for a 1465 W air conditioning unit was designed, manufactured, and tested. The compressor utilized steam created by an electric boiler to create mechanical work on an ultra-strength high temperature silicone elastomer. The mechanical work needed to create a pressure difference of 433 kPa to compress the R134a refrigerant (← read this sentence). The amount of work on the diaphragm was calculated to be 145 W, which would be theoretically achieved at a frequency of 1 Hz. A solenoid valve was opened for 0.5 seconds and closed for 0.5 seconds, in order to control the flow of steam at the aforementioned frequency. Testing yielded a max compression power of 70 W, which is an overall efficiency of 1.02%, before rupturing of the diaphragm occurred. In due course, high cyclic loading degraded the material properties of the elastomer, which ultimately caused it to catastrophically rupture.

Table of Contents

- Abstract..... 1
- Background 3
- Concept Selection 4
- System Overview – Functional Analysis..... 5
- Determining Compressor Parameters 6
- Refrigerant selection..... 8
- Advantages and Disadvantages of R134a 10
- Design and Selection of Components 11
- Control Circuit 14
- Model Verification and Prototype Testing..... 16
- Failure Modes of Diaphragm 25
- Desired Solar Power..... 27
- Recommendations for Future Development 29
 - Material Property Testing 29
 - Valve Configuration 30
 - Active Feedback Control 30
- Works Cited..... 31
- Bill of Materials 32
- Appendix 33

Background

Air conditioning accounts for a large fraction of household energy costs. The compressor unit is a major component of an HVAC system, which consumes a high amount of power. If a compressor could be developed that is powered by a readily available sustainable energy source, then energy costs could be reduced.

The project sponsor has conceptualized a compressor that is driven by high-pressure steam. The function of a compressor in a refrigeration system is to raise the pressure and temperature of a refrigerant fluid. The concept for the compressor is to transfer energy from steam, which can be produced using a concentrating solar collector, to a refrigerant fluid.

The invention consists of a pressure vessel with two chambers that are separated by an elastic membrane. In one chamber steam is to be admitted from the source. This will fill the chamber and cause the membrane to expand. The opposite chamber will contain the refrigerant fluid. As the membrane expands, the volume on the refrigerant side will decrease, and it will be compressed.

Using check valves, the flow of refrigerant will be constrained to one direction through the system. The steam being admitted to and vented from the chamber will be controlled by solenoid valves. In this way, the pressure on the steam side can be regulated and the device made to reciprocate at a specified frequency (Peacock).

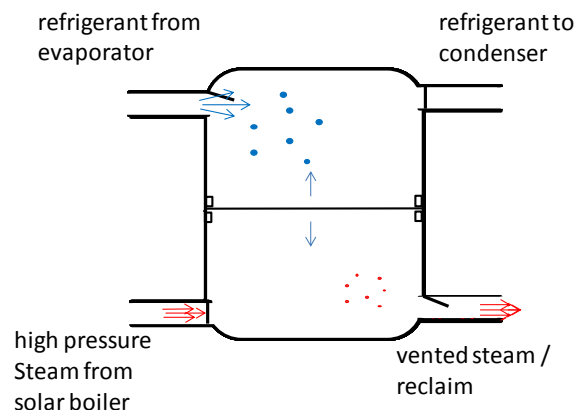


Figure 1: Concept for two-chamber compressor

Concept Selection

A device must be designed that converts energy from the sun to mechanical work. Systems that accomplish this task fall into two main types: photovoltaic and concentrated solar steam. The first is prevalent on the consumer market. Using photovoltaic panels to convert insolation to electricity, which can easily be stored and used on-demand to power a device with mechanical output is no new concept. A preliminary cost analysis was conducted which found that the PV panels required to power a small air conditioner day round would cost approximately \$13,000. A solar thermal system would potentially much less expensive. (Bender et al.)

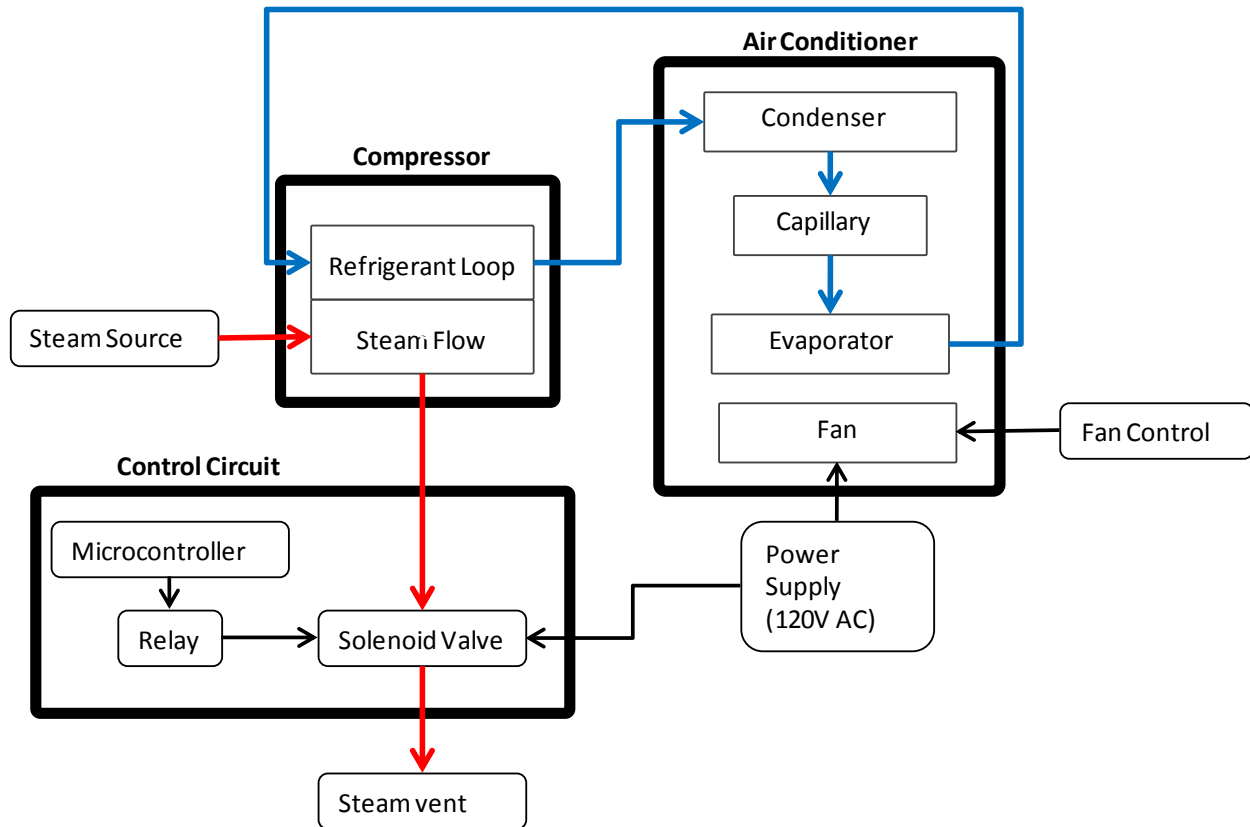
The second type of system which could potentially be used achieve our goal is solar-thermal. In such a system, concentrated solar energy is typically used to heat water and create steam. This concept has been applied to large-scale power generation. The steam is used to drive turbines and generate electricity. A subcategory of this system would use the steam to do mechanical work rather than first converting to electricity. The flow of steam can be controlled and used to compress a volume of refrigerant, as in Mr. Peacock's concept.

Two methods of implementing this concept were theorized. The first is a rigid piston that separates two variable-volume chambers. A piston-cylinder configuration would hold up well in high-temperature, high-pressure conditions. A well-designed piston would be able to undergo high-frequency cycling with minimal fatigue effects. The downside of this design is that precision machining is required. The piston must be able to move with little resistance, but must also have a seal that does not allow mixing of the fluids that it separates.

The second approach to the two-chamber concept is to use a non-permeable elastic membrane. Such a component would prevent mixing of the fluids and does not require as precise machining of the bore. A smaller displacement volume is possible for a given bore diameter. Fatigue as a result of cyclic loading is an important consideration.

At our sponsor's request, we sought to develop the membrane concept into a prototype.

System Overview – Functional Analysis



Once the concept had been decided on, the project scope could be defined in further detail. The system being designed is comprised of three major subsystems: the compressor, valve control circuit, and air conditioner.

The compressor contains two separate fluid flows, which are mechanically coupled by an elastic membrane. The steam flow (red arrows) is supplied by a source which models a high-pressure solar-generated steam supply. A solenoid valve regulates the flow of steam, allowing pressure to periodically build up in the lower chamber of the compressor then vent to ambient conditions.

The solenoid valve is regulated by the control circuit which contains an Arduino microcontroller, solid-state relay, and the solenoid which actuates the valve. A code is uploaded to the microcontroller which controls the valve duty cycle. As the steam causes the membrane to do work on the refrigerant, it will be pumped through the air conditioner (blue arrows), which is necessary to test whether the compressor is pressurizing the refrigerant.

Determining Compressor Parameters

The primary function of the compressor is to increase the pressure of the refrigerant fluid that enters it. As a result of increasing the pressure, the temperature will also rise. Modeling the cycle as an ideal vapor-compression refrigeration cycle allows the properties of the fluid entering and leaving the compressor to be determined, in as well as the properties at the other components in the cycle. Using this model, the necessary flow rate can also be determined.

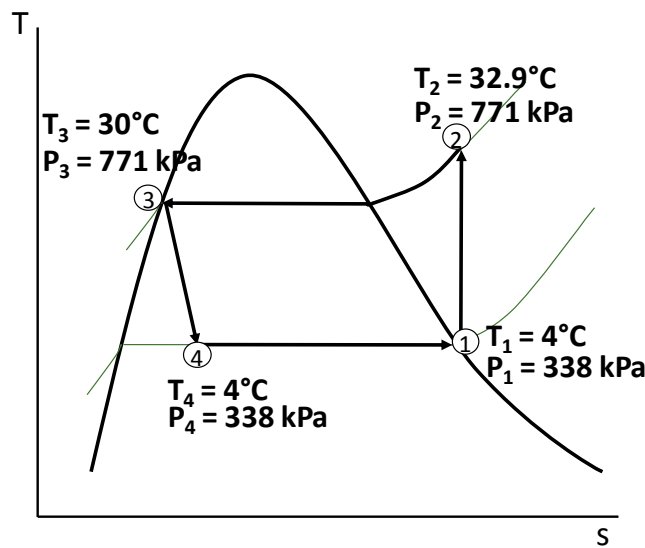


Figure 2: Ideal vapor-compression refrigeration cycle R134a

A vapor-compression refrigeration cycle contains four major components: a compressor, condenser, expansion valve, and evaporator. Within these components the following processes take place: isentropic compression (1-2), isobaric heat rejection (2-3), adiabatic expansion (3-4), and isobaric heat absorption (4-1). These four processes are superimposed onto the saturation vapor curve for R134a in the temperature-entropy graph shown above (Cengel). The reasons for the choice of R134a as the refrigerant fluid are described more in detail below (p 13).

The properties at each state can be determined beginning with the temperature at the condenser outlet (3). The function of the condenser is to exchange heat from the refrigerant fluid to the outside air. Therefore, the temperature at (3) can be no less than the outside temperature; 30°C is chosen as a reasonable daytime high temperature. Because the fluid at this point is a saturated liquid, the pressure can be determined based on the temperature, $P_3 = 771$ kPa. Neglecting pressure losses in

the condenser, process 2-3 is isobaric; so the pressure at (2) is $P_2 = 771$ kPa. This is the high pressure that the compressor must produce.

The bottom temperature limit should be as low as possible in order to maximize heat transfer from the evaporator. If 0°C was chosen, there would be a risk of water vapor from the ambient air freezing on the evaporator. A bottom limit of $T_4 = T_1 = 4^\circ\text{C}$ is chosen to mitigate this risk. Because the refrigerant entering the compressor at (1) is saturated vapor, the pressure at this point can be determined, $P_1 = 338$ kPa. Now it is specified that the compressor must raise the pressure of the refrigerant from 338 kPa to 771 kPa.

Following the process assumptions described previously, the remainder of the properties can be determined at each state. Once the enthalpies of 1 through 4 are known, the required mass flow rate can be determined. The project objective is to design a compressor for a system that can produce 1465 W of cooling. This is the heat transferred to the evaporator in process (4-1). Using $\dot{Q} = 1465$ W, $h_1 = 253$ kJ/kg.K, $h_4 = 94$ kJ/kg.K, and equation 1 below, the necessary mass flow rate is determined to be $\dot{m} = 0.009 \frac{\text{kg}}{\text{s}}$. (Bender et al.: Final)

$$\dot{Q} = \dot{m} \Delta h \quad (1)$$

Refrigerant selection

There are many refrigerants in use in air conditioning; the main refrigerants used for public air conditioning are R22, R410a, and R134a. In home air conditioning, R22 and R410a are used, while R134a is used in automobiles. As we thought up of how to build our compressor, we knew that we would be limited in how much we can compress whatever refrigerant we were using. The function of the refrigerant cycle is heat exchange; it takes in and rejects heat with the compressor moving the refrigerant. We contacted a local air conditioning repair company to get the numbers of a typical working air conditioning unit; they told us that the pressures across the condenser, the high pressure side, are between XX psi and XX psi for an R22 system. To compare these values with the other refrigerants, we use pressure-temperature charts to get the temperature of the refrigerants. Using values of weather data of Tallahassee, we estimated the temperature range outside which is where the condenser is placed. We look at refrigerant properties which give us the constant pressure specific heat of all the refrigerants we discussed above. Simple heat exchange states:

$$\dot{Q} = \dot{m} * C_p * \Delta T = \dot{m} * C_p * (T_{condenser} - T_{outside}) \quad (II)$$

Where \dot{Q} is heat transfer rate, \dot{m} is the mass flow rate, and ΔT is the difference between the refrigerant and outside temperature. We estimated that we would need the same heat transfer rate with either refrigerant so that $\dot{Q}_{R22} = \dot{Q}_{R410a} = \dot{Q}_{R134a}$, our mass flow is also the same, our specific heats are known which leaves us to solve for ΔT for which we know the outside temperature. Once the refrigerant temperatures were found, we referred once again to our pressure-temperature charts to get what pressure we need to compress our refrigerant to get the same amount of heat transfer.

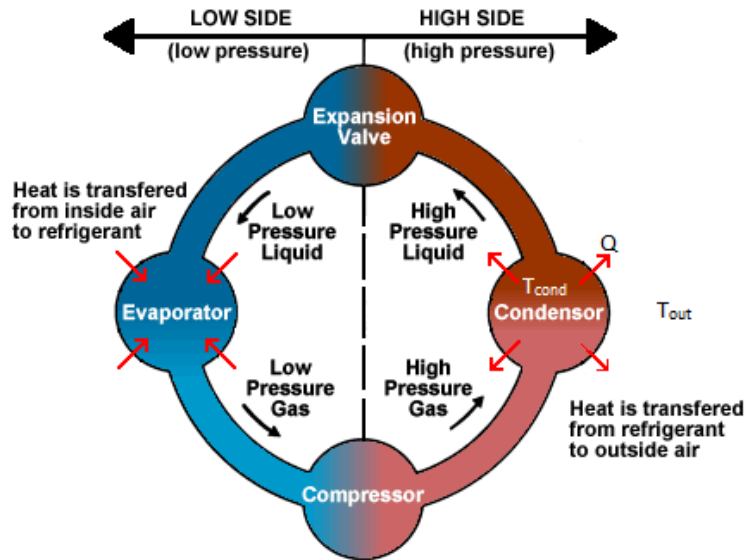


Figure 3: Refrigeration Loop for an A/C unit

We get the following table

Table 1: Refrigerant Properties

Refrigerant	Cp(kJ/kg*K)	Temperature Range(°F)	Pressure range(psi)
R22	0.65	100-120	190-250
R410a	0.87	100-120	218-274
R134a	0.84	100-120	78-104

From this we can see that it takes much less compression for R134a, than the two others. We decided that we would use R134a.

Advantages and Disadvantages of R134a

R134a requires less compression to achieve the required temperature range. Refrigerants R22 and R410a are regulated both in sales and usage primarily because of their adverse effects to the environment. R134a is a commercial refrigerant which does not require a license to purchase and the only refrigerant that doesn't require certification for usage.

Switching to a automobile refrigerant may involve the need for modifying the air conditioning unit from the normally used R22, and R410a to R134a configurations which involves changing the expansion valve (capillary tube in some models) to adjust for the effects of different properties of the refrigerants.

R134a has a safety rating of A1. This rating tells us that it has low toxicity (A) and no flame propagation (1). It has an ozone depletion potential of 0 and the lowest global warming potential among the refrigerants.

Design and Selection of Components

Membrane Design:

After the function of the compressor has been quantified, the membrane that will separate the steam from the refrigerant, and do work on the refrigerant can be designed. The theory behind the membrane is that its deflection can be predicted as a function of the properties of the material it is made from, its thickness, and the differential pressure acting on it. The formula describing the deflection of a thin, circular, elastic disk, loaded with a uniform pressure is given below (Ashby).

$$\delta = \frac{3}{16} (1 - \nu^2) \frac{P R^4}{E t^3} \quad (III)$$

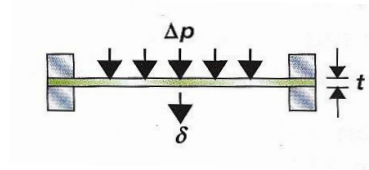


Figure 4: Circular elastic disk clamped

The approach used involved first determining the volume required for each stroke, translating this to a linear displacement δ , applying the properties of the chosen material, and solving for the required thickness. Because the displacement required to produce a specific volume depends on the radius of the membrane (a small radius requires a larger δ to produce the same volume as a large radius) the process was iterated using different values for the radius until a reasonable thickness was found.

The volume that each stroke must produce can be expressed as a function of the required mass flow rate, the density of the fluid being compressed, and the frequency of oscillation. It is proposed that a frequency, $f = 2\text{Hz}$, will be used. A higher frequency would decrease the volume required for each stroke, and this would require the membrane to be unreasonably thick. The target mass flow rate for the refrigerant is $\dot{m} = 0.009 \text{ kg/s}$, and the average density of the fluid is $\rho = 27.03 \text{ kg/m}^3$.

$$V = \frac{\dot{m}}{\rho \cdot f} \quad (IV)$$

This yields a volume per stroke of $V = 1.67 \times 10^{-4} \text{ m}^3$.

While the solenoid valves that have been selected are capable of frequencies up to 200Hz, the response of the system will depend on the flow rate of steam that is available. The system that will be

used to simulate solar steam production is capable of supplying 0.022kg/s of steam. In order to check whether the steam supply will be adequate, the same equation above is applied to the steam and solved for mass flow rate. Substituting the average density of steam $\rho = 4.16\text{kg/m}^3$, $f = 2 \text{ Hz}$, and $V = 1.67 \times 10^4 \text{ m}^3$, the mass flow rate is 0.0013kg/s, which is less than the maximum available.

The per-stroke volume is translated into a linear displacement, δ , which describes the change in position of a point on the center of the membrane. To accomplish this, the deflection of the membrane is modeled as a spherical cap, as shown below.

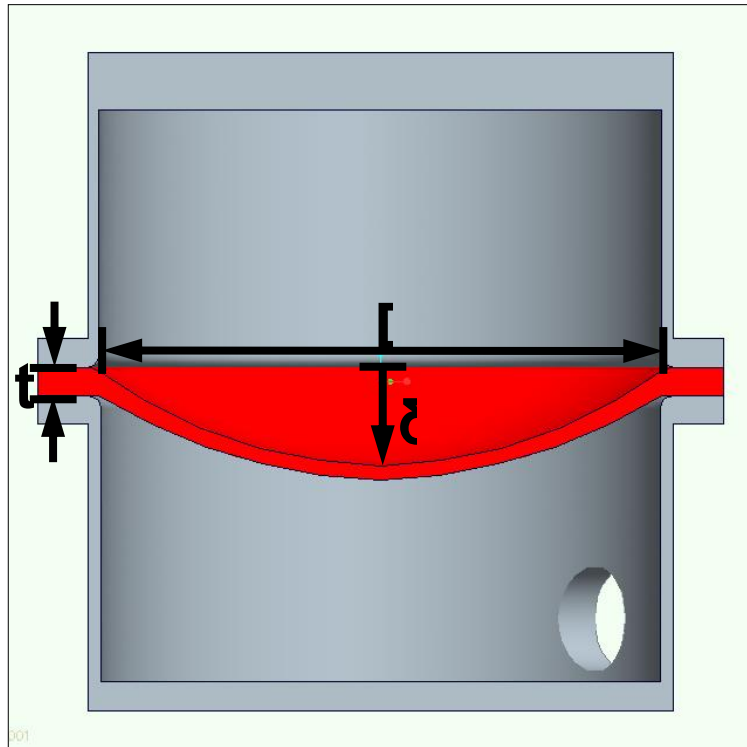


Figure 5: Volume of spherical cap

$$V_{cap} = \frac{1}{6} \pi \delta (3R^2 + \delta^2) \quad (V)$$

The radius has been chosen at $R = 0.06 \text{ m}$. This is the result of iterating the calculation until a reasonable thickness was arrived at. Equation IV above is solved for δ , using the per-stroke volume and specified radius. The maximum displacement of the center of the membrane is $\delta = 2.7 \text{ cm}$.

The final missing piece for determining the membrane thickness by equation II is Young's Modulus, E , which describes the thickness of the material. The class of materials that have been surveyed are elastomers. These were chosen first because they have a low stiffness compared to other

materials such as metals. If a metal were used for the application, its yield strength would be exceeded before the required displacement was reached. Elastomers can undergo large elastic deformation prior to yielding.

The constraint which limits the selection of a material is the high temperature environment that it must withstand. Information on the maximum temperature that various elastomers can be exposed to without degrading the yield strength has been gathered, and is summarized below.

Table 2: Maximum operating temperature of common elastomers

Material	Max T (°C)
Butyl rubber	150
Isoprene rubber	150
Neoprene	115
Polyurethane elastomer	115
Silicone elastomer	260

Silicone has a much greater temperature tolerance than the other common elastomer materials. The properties for silicone elastomer are Young's Modulus, $E = 12.5 \text{ MPa}$, and Poisson's ratio $\nu = 0.5$. Solving equation I for thickness yields, $t = 1.3 \text{ cm}$ (Bender et al.: Final).

Control Circuit

The control circuit of the phase change compressor was used to control the flow of steam. It involved multiple electrical components with the purpose of opening and closing the solenoid valve at an adjustable frequency in order to regulate the amount of steam that flowed into the compressor. The control circuit consists of a microcontroller which is responsible for ultimately opening and the closing the solenoid valve at a desired frequency. The next component in the circuit is the solid state relay, which is an electronic switching device that takes a small load input signal and transfers it to a larger load. A resistor had to be integrated between the SSR and the microcontroller in order to implement an electrical resistance to protect the circuit. To ensure that the Arduino has enough switching power a transistor was installed, which was used to amplify the electronic signal and electronic power. The relay converts the small load signal to a high load signal of the 110V solenoid valve, where the power is received from a standard outlet.

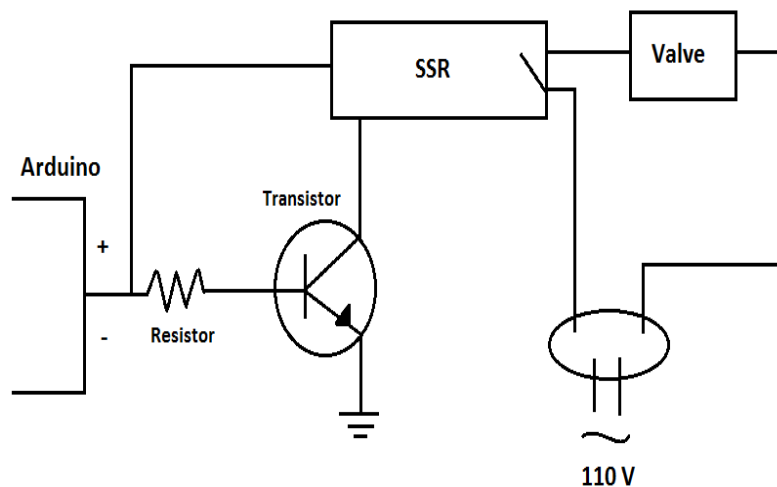
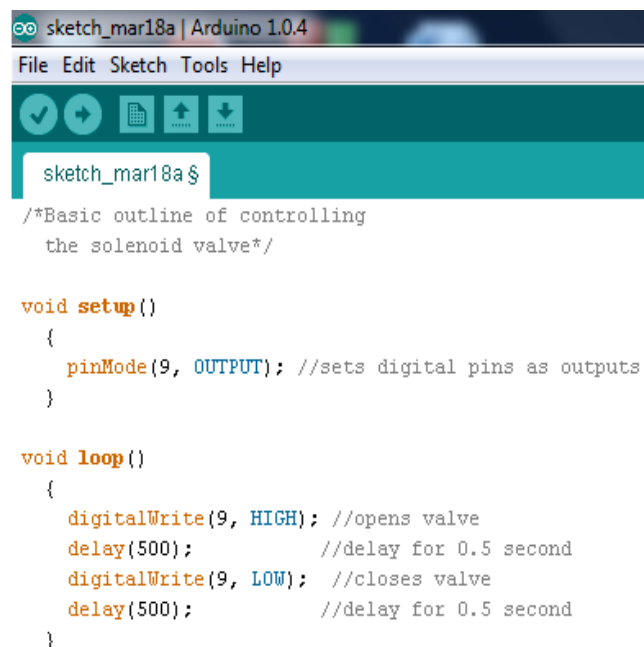


Figure 6: Control Circuit used for Operation of Solenoid Valve

The individual components of the circuit were calculated and determined based on the needs of the solenoid valve. The microcontroller was an Arduino R3 Uno, which is a small computer on a single integrated circuit containing a processor core, memory, and programmable input/output peripherals. It has an operating voltage of 5V with a 40 mA DC current per I/O pin. The relay that was selected was an Omron, industrial mount, solid state relay. It has a control voltage range between 5 and 24 volts of DC, which is compatible with the microcontroller. The load voltage by the solenoid is valve is 110 V, which falls between the rating of 19 to 264 of volts of AC. The load current of the solenoid consisted of ~80 mA which is greatly under the max of the SSR's, which is 10 A. A 2N222 Transistor was calculated by

using the properties of the operating voltage of the microcontroller, 5V. The 5.6 kΩ resistor, used to protect the circuit, was determined by Ohm's law with respect to the operating voltage and current of the microcontroller.

Overall, the control circuit was pertinent in controlling the flow of steam of the system so the system could be tested under various conditions. The electric boiler would release steam through the initial opening in the bottom chamber. The duration of the steam's presence was determined by the solenoid valve. The opening and closing of the valve at preset frequency would control the amount of pressure and oscillation onto and by the diaphragm. The selected frequency, due to aforementioned calculations needed to compress the refrigerant, was 1 Hz. This specified frequency resulted in the valve to close for 0.5 seconds; to allow for compression to occur, then would open for 0.5 seconds to decompress the diaphragm, which yielded the one cycle per second which was desired. The simple program, displayed below, was responsible for controlling the frequency from the Arduino 1.0.4 software.



```
sketch_mar18a | Arduino 1.0.4
File Edit Sketch Tools Help
sketch_mar18a $
/*Basic outline of controlling
the solenoid valve*/

void setup()
{
  pinMode(9, OUTPUT); //sets digital pins as outputs
}

void loop()
{
  digitalWrite(9, HIGH); //opens valve
  delay(500);           //delay for 0.5 second
  digitalWrite(9, LOW); //closes valve
  delay(500);           //delay for 0.5 second
}
```

Figure 7: Program used to Control Frequency of Valve

Model Verification and Prototype Testing

Testing of the prototype compressor was carried out at the FSU Energy and Sustainability Center under the supervision of John Dascomb, who provided assistance with interfacing our pressure transducer with LabVIEW. The pressure transducer was fitted to a junction in the refrigerant line on the high-pressure side of the compressor, between the check valve and the condenser. Three test routines were implemented in order to determine the capability of the designed system.

First, a static pressure test was executed to check that the system could hold the designed for pressures. An annular plate which matches the flange of the upper compressor chamber was used to clamp the membrane to the lower chamber, so that the deflection could be observed. A Schrader valve was fitted to the steam inlet valve so that chamber could be filled with compressed air. A tire pump was then used to pressurize the chamber to 65psia (448kPa). This exceeds the maximum differential pressure the membrane should be loaded by. This maximum load occurs when the compressor is in steady-state, not operating. On one side, the initial refrigerant charge in the system is approximately 400kPa; and the other side is at atmospheric pressure, 101kPa. The membrane was observed as deflecting approximately 2cm, which is in agreement with the model.



Figure 8: Initial Pressure Test of Membrane



Figure 9: Assembled Compressor

The second part of the static pressure test was performed to check whether the refrigerant loop was free from any leaks. This was necessary since several soldered connections had been made to connect the air conditioner refrigerant lines to our compressor. The compressor was assembled with the membrane clamped between the two chambers, as in the normal operating configuration. A vacuum pump was then connected to the refrigerant charging port and a vacuum of approximately 15psi was pulled on the system. The vacuum pump was removed and the pressure was monitored using the data acquisition system. After five minutes, the pressure reading remained stable, which verified there were no leaks in the refrigerant system.

The next major phase of testing applied the steam source. An electric boiler was used to simulate solar-generated steam. The temperature of the output steam was limited to 200°C in order to avoid the formation of toxic decomposition products, which occurs at temperatures in excess of 250°C (Honeywell). At this setting, the boiler was able to supply about 80psi.

The evacuated system was charged with refrigerant at 55psi. The solenoid valve was set to run at the modeled duty cycle: 1/2s open, 1/2s closed. The steam source was then turned on. As the data was monitored, the refrigerant pressure showed no fluctuation. Additionally, there appeared to be no interruption in the vented steam flow even as the valve was heard opening and closing every half second. These observations were evidence of two failures which occurred. After the steam was turned off and the compressor was allowed to cool, the membrane was removed, which revealed that it had ruptured.

A possible reason for this is that the initial refrigerant charge was too high. Also, the manner of permitting the steam to enter the chamber may have contributed to this failure. While the system was being set up for this test, the globe valve to control steam flow into the compressor was closed. Meanwhile, steam pressure was building up behind it. When this valve was quickly opened to admit the steam flow, a jet entered the chamber at higher pressure than expected. This, combined with the high temperature, caused the membrane to rupture. The material yield strength information is provided by the vendor, and the material is rated for temperatures up to 316°C (RSR). Even though these limits were not exceeded, we were unable to attain information how much the strength decreases with temperature.

The secondary failure was the valve itself. Although the manufacturer's operating conditions were not exceeded, it was determined that the valve could not fully close in 0.5s. By connecting a water hose to the valve and switching it on and off, it was found that between 1s and 2s are required for the valve to fully close.



Figure 10: Ruptured Diaphragm after Steam Test



Figure 11: Steam Exhaust through High-Temp Hose

The third test routine used compressed air, to eliminate the complications that arise as a result of using a high temperature fluid. A replacement solenoid valve was available at the ESC which had a fast enough response time for our desired frequency of operation. This valve, however, was not rated for use with steam. The diaphragm was also replaced before carrying out this test.

Improving upon the previous test, this test began with a low refrigerant charge which was gradually incremented until the designed-for pressure was reached. While a pressure transducer was used to record the refrigerant pressure, a gauge was used to observe the pressure in the bottom chamber of the compressor. The gauge was fitted at the junction between the air supply hose and the compressor. Not having sufficient refrigerant in the system would result in cooling not occurring; however, compression of the fluid could still be demonstrated.

The first test used a refrigerant charge of 202kPa. The valve was set to run at the modeled duty cycle: open for $\frac{1}{2}$ second, closed for $\frac{1}{2}$ second. During the test, the air flow was increased by incrementally opening the supply valve approximately every thirty seconds. As the solenoid opened and closed the vent, the gauge could be seen fluctuating between Opsig and a maximum pressure. The air flow was increased until the pressure reading on the gauge matched the initial refrigerant charge for each test.

This process was repeated for an initial charge of 241kPa, 290kPa, 348kPa, 448kPa, and 551kPa. Since now low-side refrigerant pressure was recorded, the total pressure increase cannot be stated with certainty. It can be said the compressor successfully increased the refrigerant pressure by at least the difference between the initial charge (P_0) and the maximum steady pressure measurement (P_H).

$$\Delta P \geq P_H - P_0 \text{ (VI)}$$

The data shows that while in steady operation, the high side pressure increases with respect to the initial charge, P_0 ; therefore, the low side pressure must be lower than the initial charge. It is conjectured that the difference between P_0 and P_H , is equivalent to the difference between P_0 and P_L .

$$P_H - P_0 = P_0 - P_L \text{ (VII)}$$

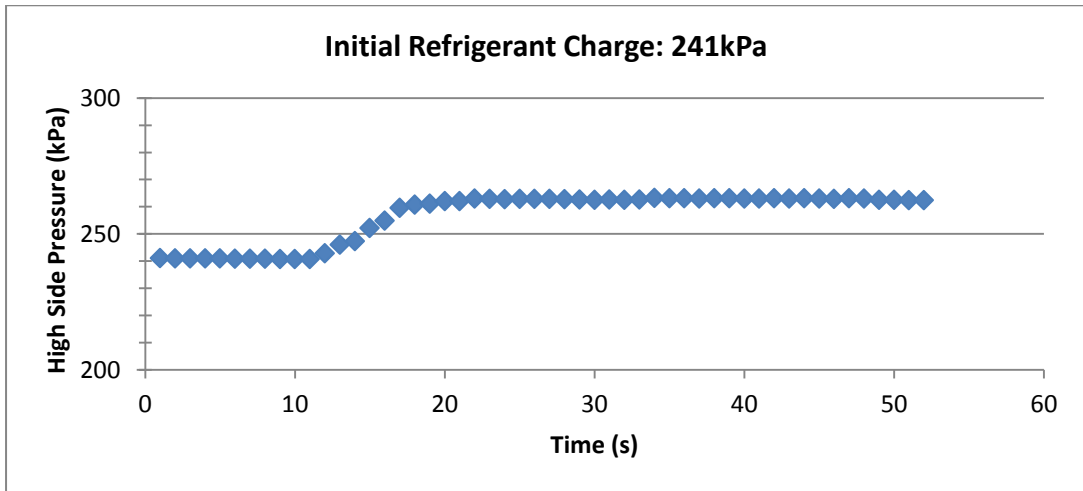
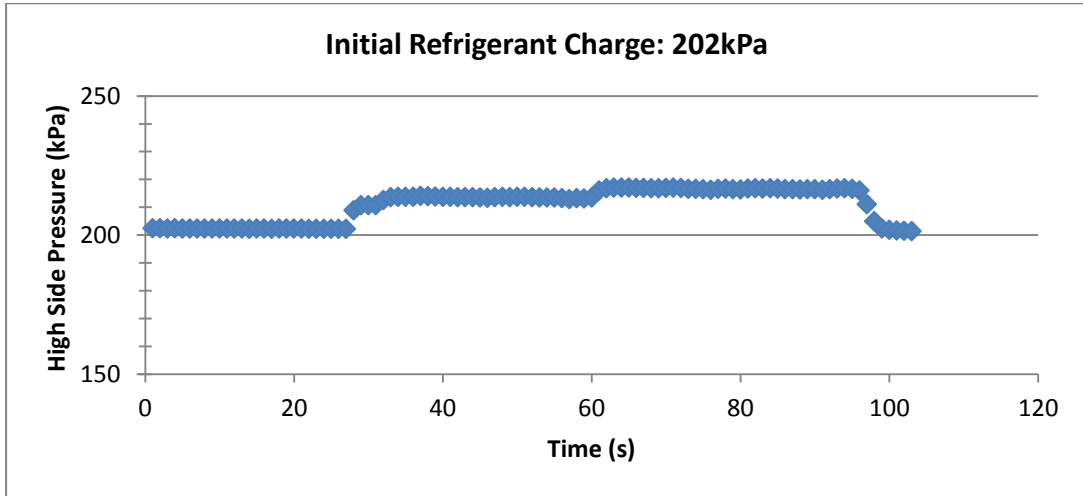
Based on this assumption, the low-side pressure can be estimated as: $P_L = P_0 - (P_H - P_0)$, and the upper limit of ΔP for each case can be estimated by the following expression:

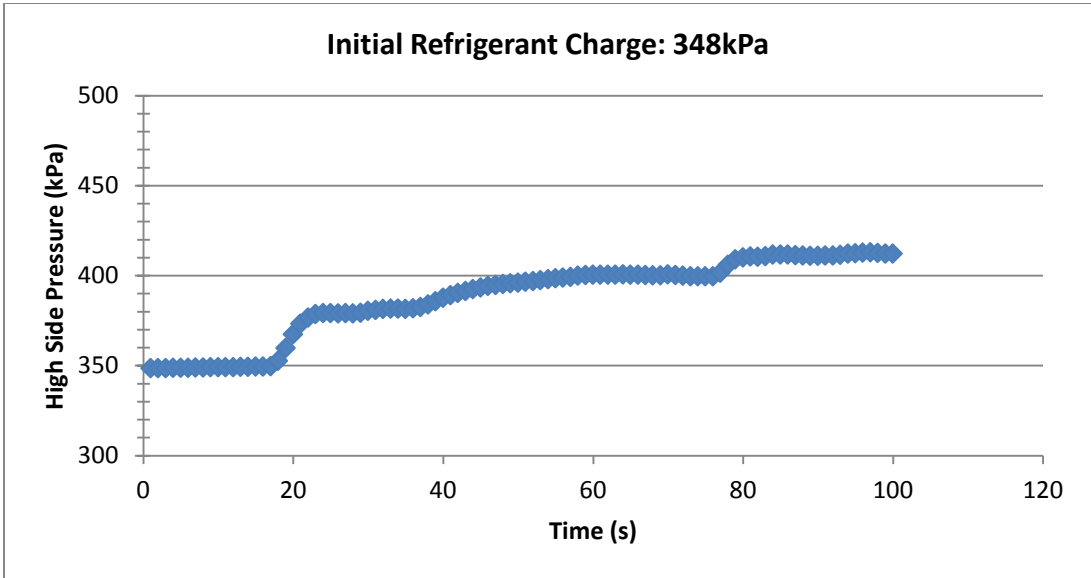
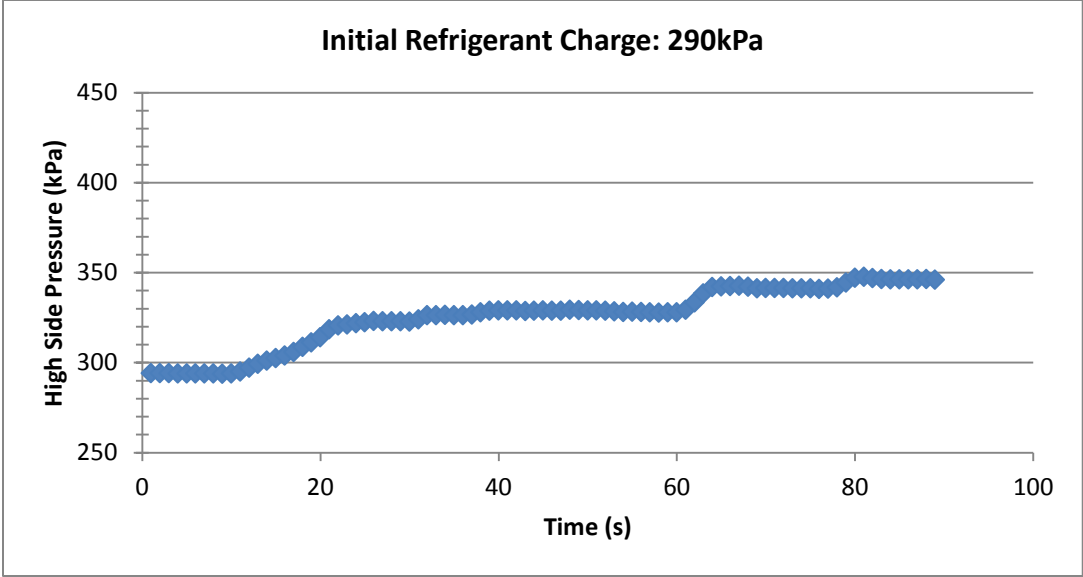
$$\Delta P \leq 2 \cdot (P_H - P_0) \text{ (VIII)}$$

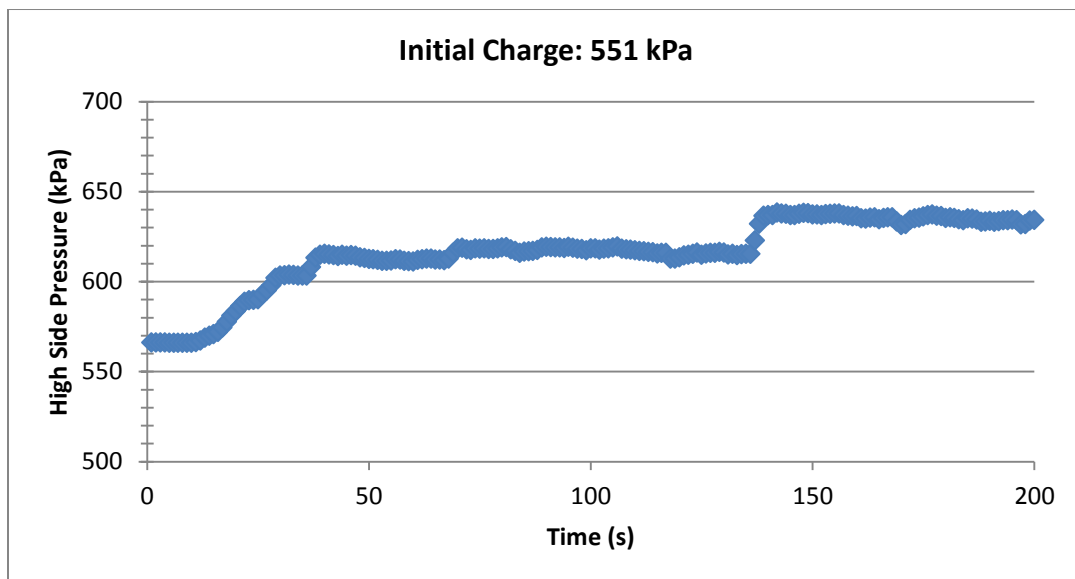
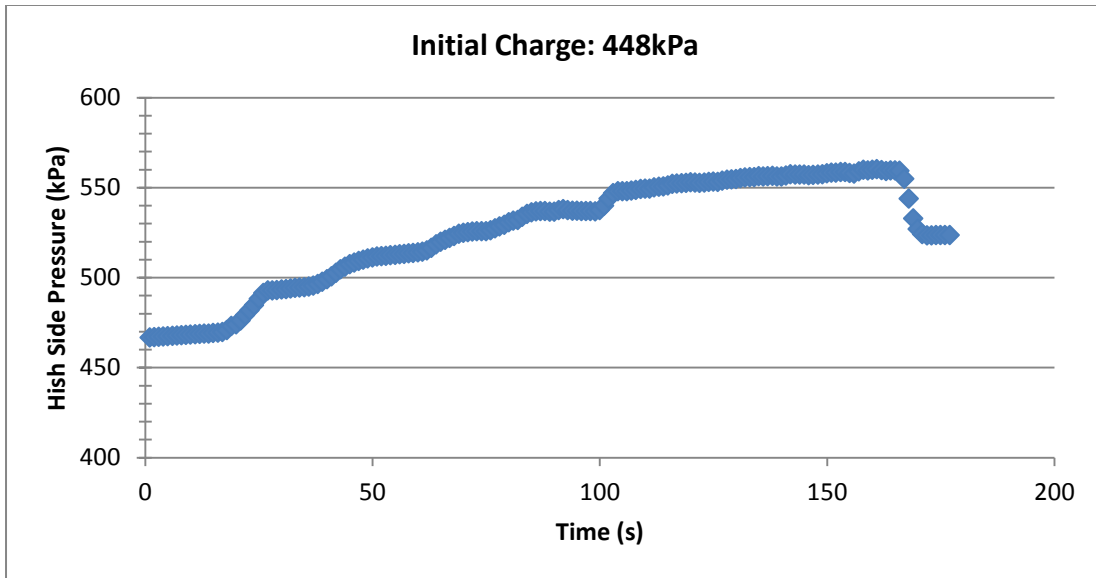
Initial Refrigerant Charge, P_0 (kPa)	High-side Pressure, P_H (kPa)	Low-side Pressure, P_L (kPa), estimated	Pressure Increase, ΔP (kPa), estimated
202	217	187	30
241	266	216	50
290	354	226	128
348	413	283	130
448	560	336	224
551	638	464	174

Keeping in mind that the model of the refrigeration cycle required $P_L = 337$ kPa and $P_H = 771$ kPa, the most successful test, in terms of ΔP , was the second to last. From an initial charge of 448kPa, the refrigerant was pressurized to 560kPa. This leads to an estimated ΔP of 224kPa, which is about half of the compression that the model predicts is necessary for refrigeration. During the final test, the membrane ruptured after a maximum steady pressure of 638kPa was achieved.

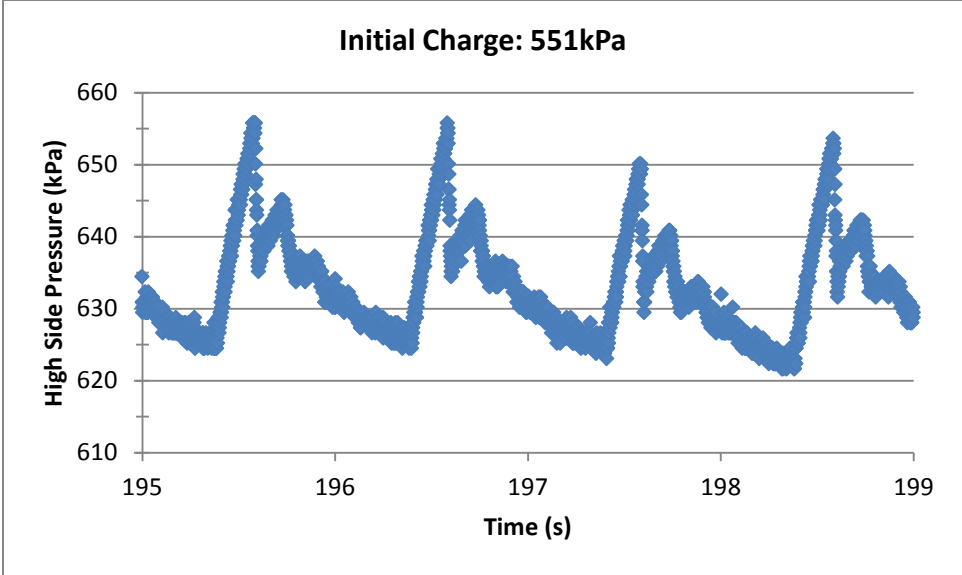
The refrigerant pressure data was sampled at a rate of 1000Hz. The following plots show the average high-side pressure reading for each second.







Within each second, there is a significant pressure fluctuation, as shown in the plot below. The solenoid valve is operated on a duty cycle that is closed for 1/2s, opened for 1/2s; thus each second shows an increasing trend followed by a decreasing trend as the valve is closed, then opens. Each sharp spike begins as the valve is closed. The pressure increases in the lower chamber, inflating the membrane. As this occurs, the refrigerant is compressed. When the control valve is opened, the membrane drops and the check valve to the high pressure side of the refrigerant loop closes. As this takes place the high-side pressure gradually falls as the refrigerant flows through the heat exchangers and capillary tube.



Failure Modes of Diaphragm

The diaphragm that was carefully selected was an ultra-strength high temperature silicone elastomer membrane. It was under heavy cyclic loading of about 3600 cycles per hour with response to the 1 Hz frequency. The membrane was also subjected to high temperatures of up to 200° C, generated by the electric steam boiler, and R-134A pressurized up to 550 kPa. The constantly changing conditions and various movements make the diaphragm prone to failure.

Elastic membranes are not commonly used in industrial applications. This is due to its various modes of failure. In the assembly of the compressor, the membrane was hand tightened between two steel chambers by nuts and bolts. If each bolt did not possess the same torque, due to the turning force of the hand onto the bolt, the force along the flange would not be equally distributed. The lack of equivalent forces would yield an inadequate seal, resulting in a minor refrigerant loss. This minor loss would decrease the overall system performance because more pressure would be needed in order to supply the system with correct amount of R-134a. The cyclic loading of the membrane due to the frequency loading would cause fatigue in the membrane. This specific loading would generate micro cracks, which would decrease the overall strength of the membrane. The propagation of the micro cracks would continuously grow due the 3600 cycles per hour of the system. These stress concentrations would be prime areas for rupturing to occur. Once the diaphragm is ruptured, major refrigerant loss is observed.

Table 3: Failure Modes of Diaphragm

Failure Cause	Failure Effect
Inadequate Seal	Minor Refrigerant Loss
Fatigue	Decrease in Material Strength
Inadequate Strength Characteristics	Major Refrigerant Loss

Overall, the high cyclic loading of the system was the downfall in the system. Further investigation on selecting a membrane must be done in order to prevent failing. Testing the current membrane for failure characteristics, due to fatigue, which is not given by manufacturer, is another

solution in assisting to have a working system. The rupturing of the membrane, as seen below is a condition that must be further studied if progress of the phase change compressor is to occur.

Desired Solar Power

To satisfy the complete design of a solar powered phase change compressor, a steam generation system must be analyzed in order to understand the feasibility of the system in the real world. To generate steam, through solar power, a concentrated solar collector (CSC) will be used for calculations, due to its prevalence in the industry. A CSC is a parabolic highly reflective dish that concentrates the sun's insolation to a receiver/boiler. The heat is focused on the receiver, which has medium is a sodium nitrate salt that possesses a large heat capacity. Water is then pumped through the receiver in order to transfer heat. The heated water is then flash boiled through a large pressure drop, which is then focused into the lower chamber of the compressor.



Figure 12: Concentrating Solar Collector

To calculate the necessary steam generating components, an analysis of the compression power needed to push the refrigerant through the system is needed. To determine the power needed, the formula, $\dot{W} = \int P dV$, is used. The differential pressure needed is 433 kPa and the volumetric displacement of the membrane is $3.34 \times 10^{-4} \frac{m^3}{s}$, which yields a power of 145 W. Through industry standards of CSC and conversion processes, a dish size of 6.47 m^2 must be desired to yield the theoretical 970 W of thermal energy needed. The actual compression pressure observed was 265 kPa, which yielded 70 W of mechanical power by the diaphragm. The overall efficiency of the actual system, which is the $\frac{\text{Compression Power}}{\text{Solar Insolation}}$, yields 1.0%. This is respect to the 6890 W generated by the 6.47 m^2 dish.

Since the system did not compress the refrigerant, due to rupturing, a successful test was not observed. The following table displays the values needed if the diaphragm could withstand the working

environment. Due to the decreased compression power, the dish size would have to be increased to 13.39 m² in order to generate the 145 W of mechanical output in order to have a successful design.

Table 4: Desired Solar Power Data

	Theoretical	Actual	
Compression Power	145 W	70 W	
Dish Size Required	6.47 m ²	13.39m ²	Extrapolated
Thermal Energy Needed	970 W	2,007 W	
Overall Efficiency	2.1%	1.0%	
\$/Watt	9.63	19.93	

The feasibility of the system is very low due to many factors. The high cyclic loading of the diaphragm must either be significantly decreased or a different material must be implanted in order to prevent catastrophic rupturing. Another important is the price of the overall system in order to power a 5000 BTU/hr Air Conditioning wall unit. Without the cost of the CSC, the price per watt of the PCC was approximately \$20/Watt. Without the cost of installation of Photovoltaic panels, the price per watt figures to be (\$1-\$3)/Watt determining on whether or not purchased in bulk. Overall, even if a working diaphragm is implemented, the cost of the system must be drastically reduced in order to have a competitive system in the market.

Recommendations for Future Development

Material Property Testing

Further development of this design requires a more thorough understanding of the material properties of the membrane material. Material property databases report the Young's modulus of silicone elastomer is between 5 MPa and 20 MPa (Ashby). The actual value of this property for the material purchased was not provided by the vendor. The yield strength of the material used must also be pinpointed so that the actual stress in the material does not exceed this value. The yield strength of high-temperature silicone elastomer is reported as 6.6MPa to 8MPa (Primasil). Poisson's ratio is reported as 0.47 to 0.49 (Azom).

According to the model used to predict the deflection of the membrane under a steady-state pressure load, the maximum stress in the material is defined by the following equation.

$$\sigma_{max} = \frac{3}{8}(1 + \nu) \frac{\Delta P R^2}{t^2} \quad (IX)$$

For the upper limit of Poisson's ratio, and the designed parameters (R = 6cm, ΔP = 450kPa, t = 1.27cm) the predicted maximum stress is 5.6MPa. This, however, does not take into account the effects of fatigue or extended exposure to high temperature.

The model used to design the prototype specifies the frequency of reciprocation at 1 Hz. Assuming that the compressor is running for twelve hours per day, the membrane undergoes 43200 oscillations per day. It is expected that the yield strength will degrade with cyclic loading and increased temperature. As elastomers are repeatedly loaded, cracks form on a microscopic scale which eventually propagate and lead to failure (Axel). Though the elastomer used in the current prototype is designated "high temperature", and is described as being able to withstand 274°C, it is unclear how the properties respond to these conditions. It is possible that the strength degrades at temperatures near this limit.

For continuing work, it is recommended that a test rig to simulate the operating conditions of the compressor be developed. The primary focus would be to gather data on how the membrane strength degrades with the number of cycles. Different materials could be tested at realistic temperatures to determine their usefulness for this application.

Valve Configuration

The original design for the compressor included two control valves for the steam: one at the inlet, and one at the vent. As the design evolved, it was decided to use only one valve at the vent for reasons of simplicity and improving reliability. It was proven that the compressor can function with this configuration; however, it is not energy efficient.

When the vent is opened to release the steam pressure, the supply steam continues to flow. As this occurs, the energy that was used to increase the pressure and temperature of the steam is wasted. Implementing a second control valve at the steam chamber inlet that closes as the vent is opened would mitigate this loss. For a 50% duty cycle, the overall energy consumption with respect to the one-valve design would be reduced by half.

Active Feedback Control

In order to ensure a robust system that is capable of producing the required output in a variety of conditions active control can be implemented in a future prototype. The system should be able to respond to small fluctuations in the steam supply. Ideally, multiple sensors would be used to monitor the high and low-side refrigerant pressure, in addition to the steam pressure and flow rate. These sensors could provide feedback to a controller that could adjust the control valve duty cycle if the target compression is not being achieved.

Works Cited

- Ashby, Michael. *Material Selection in Mechanical Design*. 4th ed. Butterworth-Heinemann, 2011.
- Axel Products, Inc. *Elastomeric Fatigue Property Mapping*. 18 Apr 2013.
http://www.axelproducts.com/downloads/Elastomer_Fatigue_Property_Map_Pricing.pdf
- Azom: The A to Z of Materials. *Silicone Rubber*. 18 Apr 2013.
<http://www.azom.com/properties.aspx?ArticleID=920>
- Bender, Addison; Diaz, Jesse; Ferdinand, Emmanuel. Final Design Report – Fall Semester. 2012.
http://eng.fsu.edu/me/senior_design/2013/team20/Final%20Report%20Team%2020%20rev2.pdf
- Bender, Addison; Diaz, Jesse; Ferdinand, Emmanuel. Operation Manual. 2012.
http://eng.fsu.edu/me/senior_design/2013/team20/Operational%20Manual.pdf
- Bender, Addison; Diaz, Jesse; Ferdinand, Emmanuel. Conceptual Design Review. 2012.
http://eng.fsu.edu/me/senior_design/2013/team20/concept%20report.pdf
- Cengel, Yunnus; Cimbala, John; Turner, Robert. *Fundamentals of Thermal-Fluid Sciences*. 4th ed. New York: McGraw-Hill. 2012.
- Dascomb, John, "Low-Cost Concentrating Solar Collector for Steam Generation" (2009).*Electronic Theses, Treatises and Dissertations*. Paper 833. <http://diginole.lib.fsu.edu/etd/833>
- Honeywell. *Material Safety Data Sheet:134a/1234ze(E)*. 6 Sep 2011. 22 Apr 2013.
http://www.honeywellmsds.com/ehswww/hon/result/report.jsp?P_LANGU=E&P_SYS=1&P_SSN=1693&P_REP=00000000000000000001&P_RES=407
- Peacock, Grant. "Phase Change Compressor". Patent 20,100,192,568. 5 Aug 2010.
<http://www.google.com/patents/US20100192568?pg=PA1&dq=grant+peacock&hl=en&sa=X&ei=jViiUOT4H4PY8gT2i4CoBQ&ved=0CDEQ6AEwAQ#v=onepage&q=grant%20peacock&f=false>
- Primasil Silicones. *High Temperature Silicone Rubber*. 18 Apr 2013.
<http://www.primasil.com/en/content/cms/home/silicones/products-services/material-formulation/high-temp-silicone/>

Bill of Materials

Item	Vendor	Item #	Price
Microcontroller: Arduino Uno R3	Radio Shack	276-128	29.99
ASCO Solenoid Valve	Grainger	4NWZ8	312.5
High Temperature Silicone Rubber, 3/8"	Rubber Sheet Roll		113.56
Extreme Temperature Silicone Rubber, 1/4"	McMaster-Carr	8632K46	26.55
6"x6" Steel Cylinder	McMaster-Carr	7786T78	155.82
High-use check valves (x2)	McMaster-Carr	4894K47	105.24
Globe Valve	McMaster-Carr	47865K43	11.18
Ashcroft Pressure Transducer	Grainger	5DEK4	175.5
1/8" copper tee	McMaster-Carr	5520K833	3.89
Refrigerant clamp-on valve (x2)	McMaster-Carr	1809K28	14.54
Low-pressure steam hose, 3/4" NPT	McMaster-Carr	5301K22	83.98
Reducing Coupling, 1/4"MNPT x 1/8"FNPT	McMaster-Carr	5520K221	1.01
Copper tube, 1/8"	McMaster-Carr	8967K883	5.84
Refrigerant service manifold	McMaster-Carr	1873K32	174.5
PTFE pipe thread tape	McMaster-Carr	44945K12	6.12
Reducing Adapter, 1/4"FNPT x 1/8" Female C	McMaster-Carr	5520K174	4.04
Reducing Adapter, 1/2"MNPT x 1/4" Female C (x2)	McMaster-Carr	5520K493	4.12
Reducing Adapter, 1/2"MNPT x 3/8" Female C (x2)	McMaster-Carr	5520K502	5.4
Adapter, 1/8"Female C x 1/8"FNPT	Grainger	1VLR7	5.7
Pressure relief valve, 1/2"MNPT	McMaster-Carr	4755K11	143.3
Solid State Relay,	Mouser	653-G3A-210B-DC5	15.3
Straight Blade Plug, 120V,15Amp-ac	Grainger	1PKF8	16.44
M to F Jumpers and Headers	Radio Shack	276-156	6.99
Compound Gauge, 1/4" Ctr Back, 30"hg-0,200 Psi	McMaster-Carr	4004K72	12.07
Reducing Bushing, 1/2"MNPT x 1/4"FNPT	McMaster-Carr	50785K65	2.54
Air Fill Valve, 1/4"MNPT	McMaster-Carr	8063K37	3.94
Window Unit AC, 5000btu	Quick Appliance		102.13
Elbow, 1/2"FNPT	Home Depot		1.64
Street Elbow, 1/2"MxFNPT (x3)	Home Depot		7.02
Nipple, 4-1/2", 1/2"MNPT	Home Depot		1.87
Nipple, 1-1/2", 1/2"MNPT (x2)	Home Depot		2.68
Nipple, 2", 1/2"MNPT	Home Depot		1.34
Coupling, 1/2"FNPT	Home Depot		1.97
Copper Tube, 3/8", 10'	Home Depot		13.48
Refrigerant Port-Quick Connect Adapter	Auto Zone		12.99
Modular IC Breadboard Socket	Radio Shack	276-003	9.99
Transistor 2N222	Radio Shack		1.49
Resistor 5K Ohm	Radio Shack		1.49
Nipple, 1-1/2", 3/4"MNPT	Home Depot		1.58
Refrigerant R134a, 12oz (x2)	Auto Zone		29.98
		Total:	1629.71

Appendix

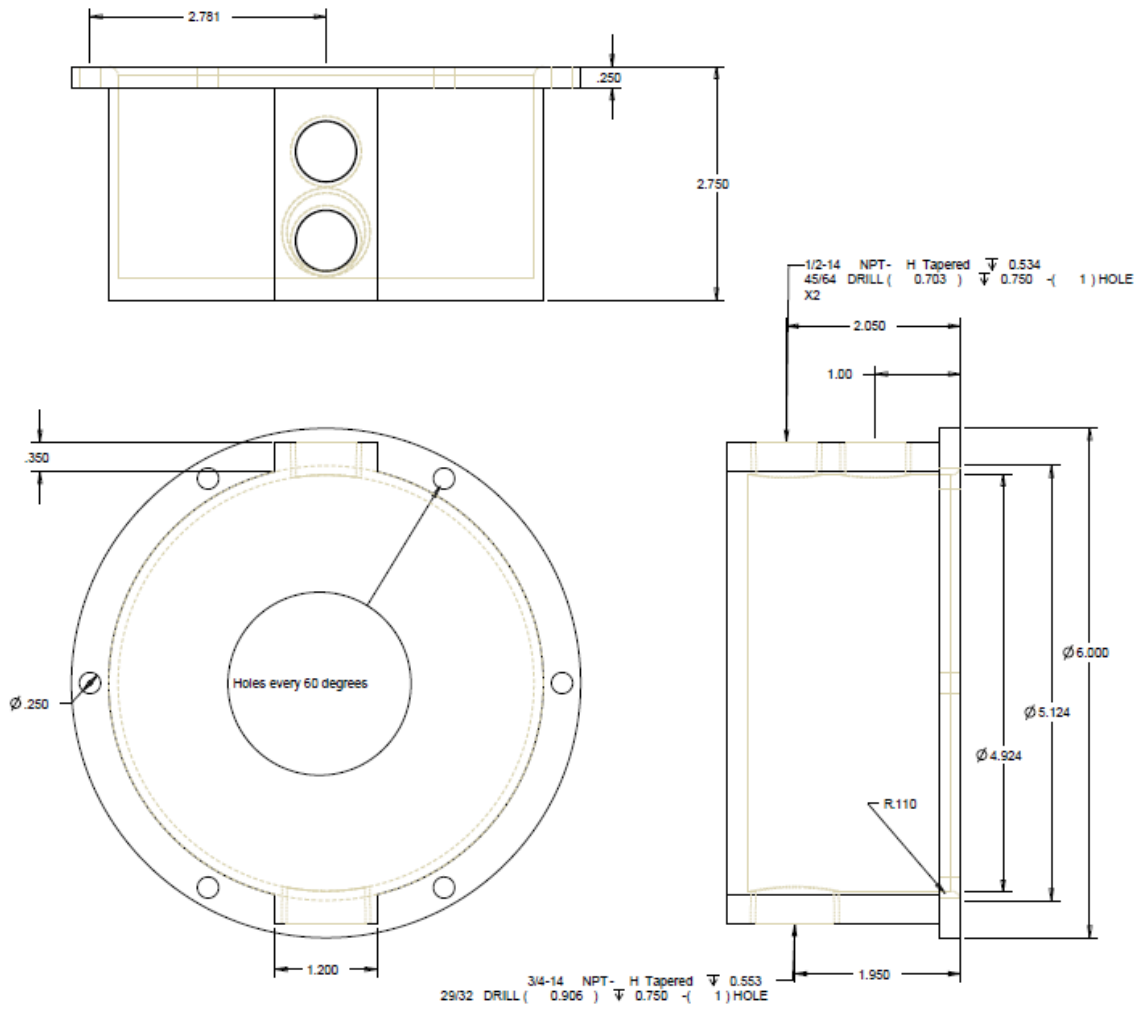


Figure 13: Compressor Steam Compartment

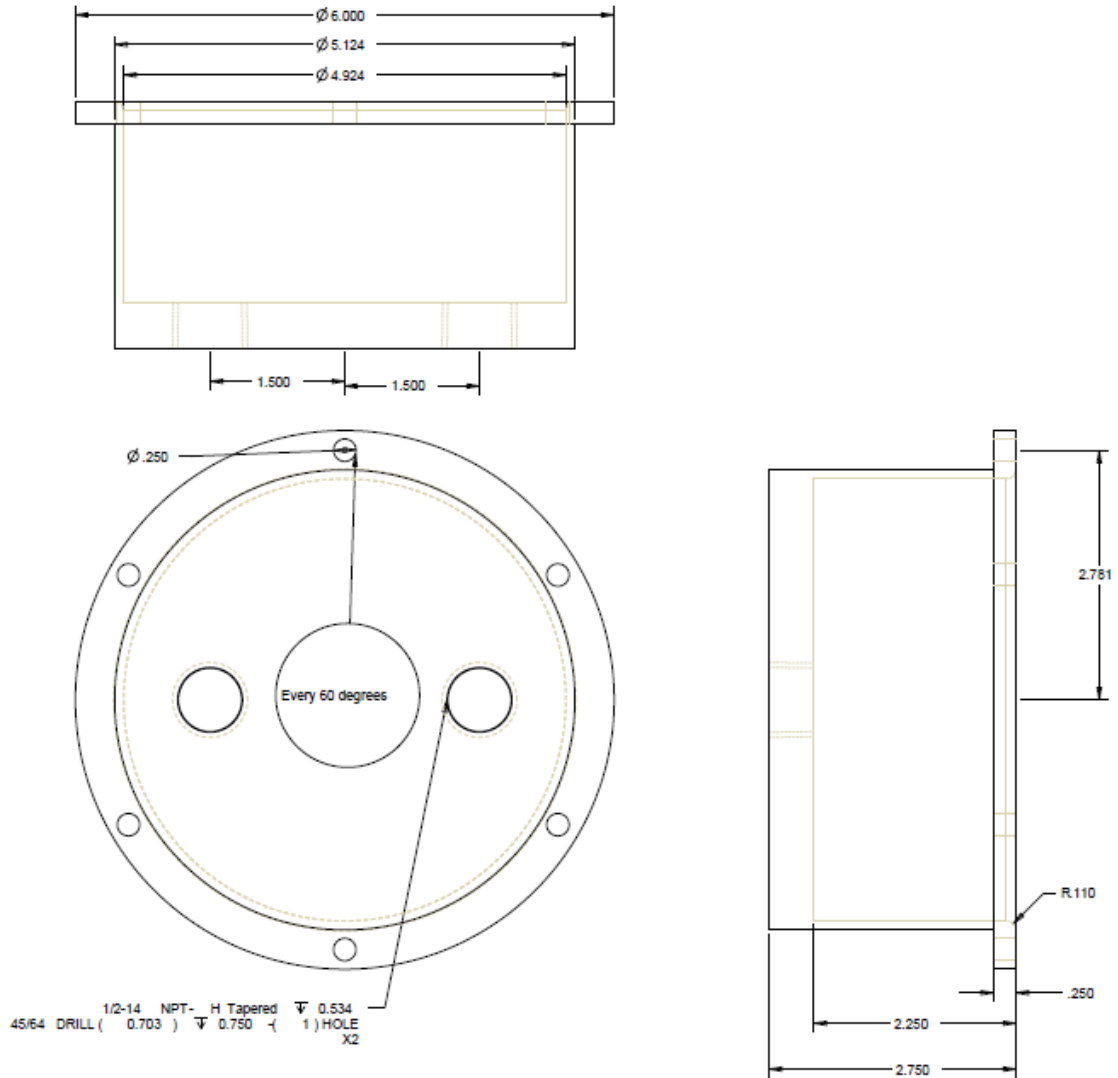


Figure 14: Compressor Refrigerant Compartment

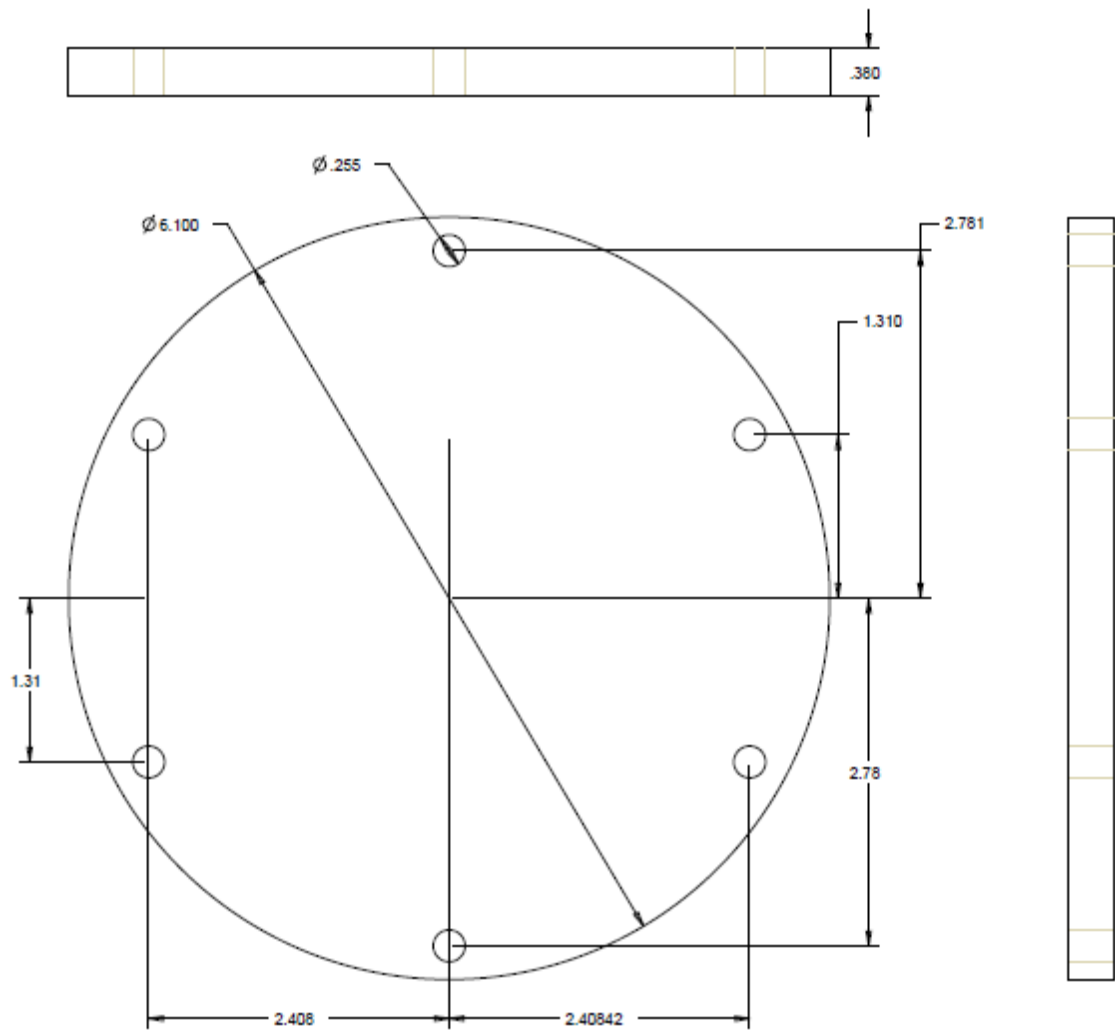


Figure 15: Membrane

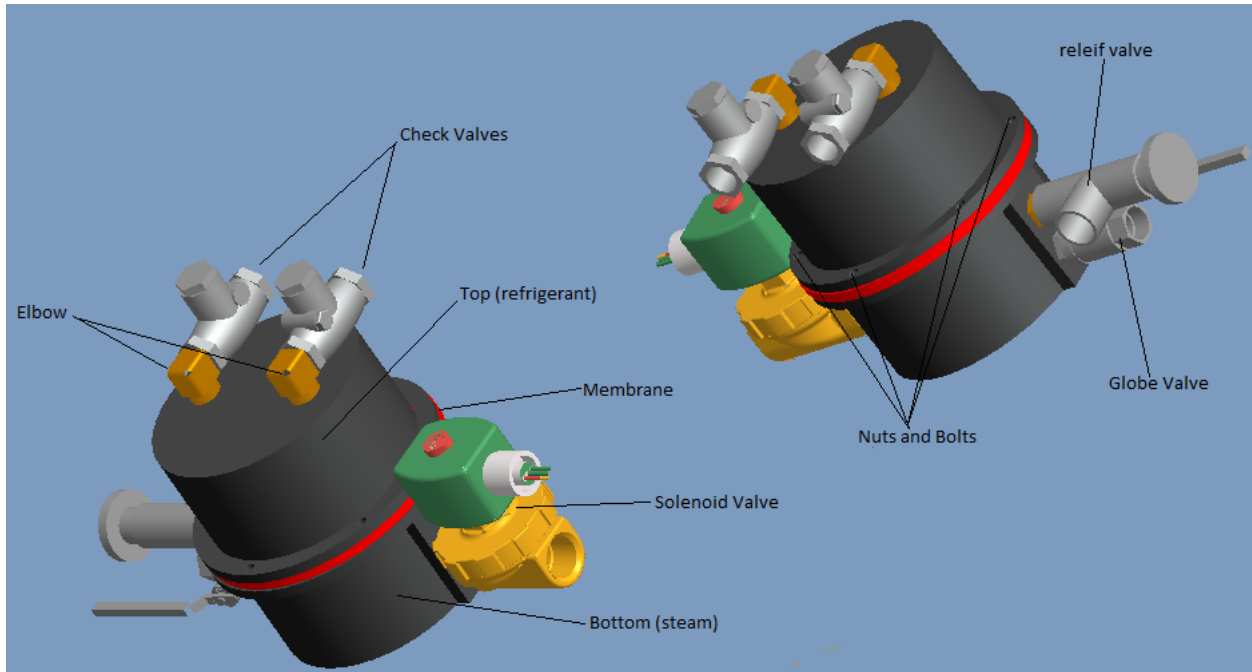


Figure 16: Completed Assembly

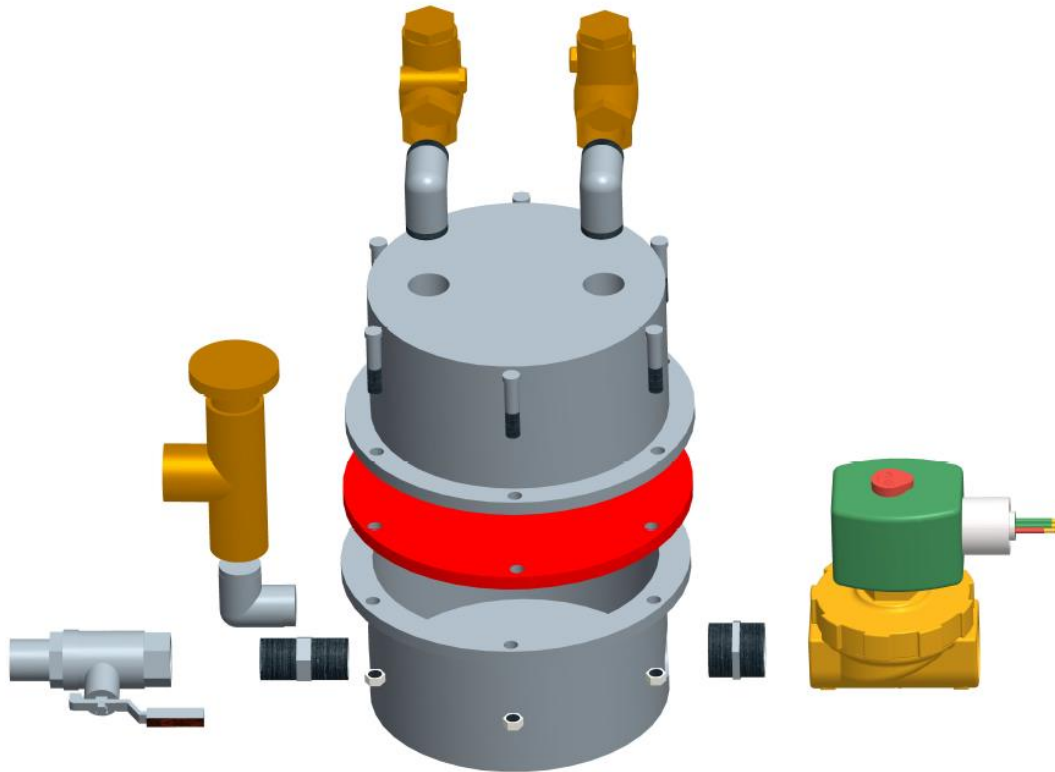


Figure 17: Exploded View